Decarburization and Chromium Conservation Model in AOD Refining Process of 304 Stainless Steel

Jun Cai and Jing Li

Abstract Decreasing chromium loss in the decarburization stage of the argon oxygen decarburization (AOD) refining process is one of the key technologies of 304 stainless steel smelting. In this paper, based on the theoretical conditions and production status of a 75 t AOD furnace, a decarburization and chromium conservation mathematical model of 304 stainless steel was established. Using this model, conditions of chromium oxidization in different situations can be predicted, and the required CO partial pressure as well as the gas supply parameters of decarburization and chromium conservation under different smelting conditions can also be calculated. Applying the model on a 75 t AOD furnace, the side and top combined blowing parameters in AOD refining process were optimized, and the burning loss of chromium in molten steel was also reduced obviously. In addition, a 379.2 kg decrease of the average consumption of ferrosilicon in the reduction stage has been achieved using the model, and the average smelting cycle was shortened by 6.4 min.

Keywords Decarburization and chromium conservation model · Argon oxygen decarburization · 304 stainless steel

Introduction

Nowadays, approximately 70% of world's stainless steel is produced through the electric arc furnace (EAF) → argon oxygen decarburization (AOD) process [1]. Due to the relatively high carbon content of austenitic stainless steel, to speed up the smelting rhythm, most production enterprises adopt this process [2–5]. As a typical austenitic stainless steel, 304 stainless steel is widely used owing to the characteristics of corrosion resistance, low temperature plasticity, easy forming, and good weldability. As one of the key links, AOD refining process directly affects the molten steel quality and cost-effectiveness of 304 stainless steel, such as burning loss

J. Cai · J. Li (✉)
State Key Laboratory of Advanced Metallurgy, University of Science and Technology Beijing, Beijing 100083, China
e-mail: lijing@ustb.edu.cn

Z. Peng et al. (eds.), *12th International Symposium on High-Temperature Metallurgical Processing*, The Minerals, Metals & Materials Series,
https://doi.org/10.1007/978-3-030-92388-4_7

of chromium [6] and ferrosilicon consumption [7]. Moreover, the decarbonization efficiency in AOD refining process has a significant influence on the smelting cycle, which is considered as an essential impact of operation-level performance [8].

During the research work of the past few decades, many mathematical models in AOD refining process of stainless steel production were established, such as decarburization rate [9], heat balance calculation [10], and temperature prediction [11, 12], which have also been applied to industrial production successfully [13]. However, few works about the decarburization and chromium conservation model in the AOD refining process of 304 stainless steel were reported, especially the dynamic control of decarburization and chromium conservation by determining blowing parameters through model calculation. For different initial molten steel conditions, as the blowing goes on, the temperature and composition of molten steel were different and changed dynamically at different blowing periods. Correspondingly, these differences caused a change kinetic and thermodynamic conditions of the decarburization and chromium conservation, furthermore, greatly affects the quality control of 304 stainless steel in AOD refining process. Therefore, the establishment of decarburization and chromium conservation calculation model is complex and is of great significance for the actual production of 304 stainless steel. Based on the actual operations, thermodynamic and kinetic conditions of the blowing process of refining 304 stainless steel in the 75 t AOD converter, a mathematical model of molten steel decarburization and chromium conservation in the decarburization process of 304 stainless steel was established in this paper. According to determined conditions of initial molten steel and blowing parameters, the model can be used to judge whether chromium burning loss occurs, calculate and determine the relative process parameters for controlling chromium burning loss. Moreover, through using the calculation results of the model, the gas supply parameters required for the molten steel decarburization and chromium conservation were determined in the decarburization stage of the AOD refining process. Combined with the mathematical model of decarburization and chromium conservation and the actual operating conditions of the 75 t AOD converter refining 304 stainless steel, the purpose of decarburization and chromium conservation in the decarburization stage was achieved by adjusting the gas supply parameters, and the burning loss of chromium in molten steel was minimized, which has essential guiding significance for the optimization of gas supply parameters in the actual production process of 304 stainless steel.

Establishment of Decarburization and Chromium Conservation Model

Process Introduction

In this paper, the 304 stainless steel is produced by the process of EAF → AOD → LF (Ladle Furnace) → CC (Continuous Casting), and the process schematic diagram is shown in Fig. 1.

The decarburization and chromium conservation model was established on the basis of the refining of AOD refining process of 304 stainless steel. The mixture of inert gas and oxygen was blown into AOD refining furnace through side–top combined blowing, in which oxygen is mainly used for decarbonization and inert gas (argon or nitrogen) is mainly used to reduce the partial pressure of carbon monoxide. AOD refining process can be divided into four stages, namely steel melting stage, decarburization period I, decarburization period II, and reduction stage. Before the reduction stage, nitrogen is used to replace expensive argon, and pure argon is blown on the side in the reduction stage. In the steel melting and decarburization stage, due to the side–top combined blowing and six branch gas supply, the gas stirs the molten bath strongly, and the dynamic conditions are good.

In the steel melting stage, the initial molten steel, slag, scrap, alloy, and other furnace charges are mixed into the AOD furnace. Because of high contents of carbon and silicon in the initial molten steel and a low molten bath temperature, pure oxygen and the mixture of oxygen and nitrogen are blown into AOD refining furnace to heat up the bath rapidly through top blowing and side blowing, respectively. In the actual production process, in order to protect the side blowing elements, furnace lining, and safe production, a certain flow of nitrogen (>16 Nm/min) is necessary to be blown as the protective gas through side blowing, and the maximum value of R, the mass ratio of oxygen to nitrogen, is 8.5.

The decarburization stage includes decarburization period I and II. The side–top combined blowing process is adopted for decarburization, and the gas supply parameter R can be adjusted online. As the progress of decarburization reaction progresses, the carbon content in steel gradually decreases, and the bath temperature increases. When the carbon content drops to a certain value and the temperature meets the requirements, the R value is decreased to reduce metal burning loss and control the excessive temperature of the molten bath. When the decarburization stage ends

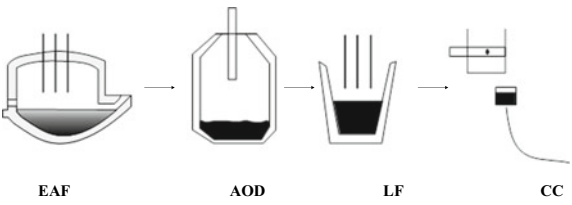

Fig. 1 Production process schematic diagram of stainless steel

and enters the reduction stage, stop top blowing and side blowing with pure argon. Moreover, alloy, lime, etc., were added into molten bath to adjust the composition of molten steel and refining slag, in which ferrosilicon was added to reduce (Cr_2O_3) in the slag to [Cr] and back to the molten steel. After the temperature and composition of molten steel meet the target requirements, the tapping operation was carried out.

Competitive Oxidation of Carbon and Chromium in AOD Decarburization Stage

In the decarburization stage of AOD refining process, based on the industrial site gas supply intensity, when the molten steel carbon concentration is high (high carbon area), the molten steel decarburization reaction rate is mainly determined by the oxygen supply intensity. When the molten steel carbon concentration is low (low carbon area), the molten steel decarburization reaction rate is mainly determined by the mass transfer rate of [C] from the molten steel to the gas–liquid reaction interface. There is a critical carbon concentration corresponding to the oxygen supply intensity. When the carbon concentration is higher than the critical value, the oxygen blown into the bath reacts with carbon without chromium burning. When the carbon concentration of molten steel is lower than the critical value, the competitive oxidation of carbon and chromium occurs, and chromium was oxidized to Cr_2O_3, resulting in the burning loss of chromium. The changing curve of conversion temperature of competitive oxidation of carbon and chromium during decarburization in AOD refining process of 304 stainless steel is shown in Fig. 2.

According to Fig. 2, in the process of competitive oxidation of carbon and chromium, the increase of [C] content and temperature are beneficial to decarburization and chromium reservation in the molten bath. As the content of [C] decreases, the conversion temperature of competitive oxidation of carbon and chromium gradually increases. When the content of [C] in molten steel is greater than 0.3%, the

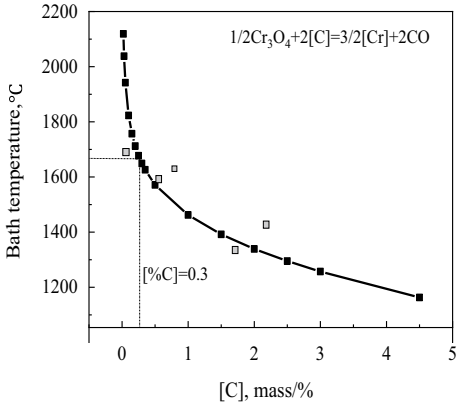

Fig. 2 Curve of conversion temperature of competitive oxidation of carbon and chromium

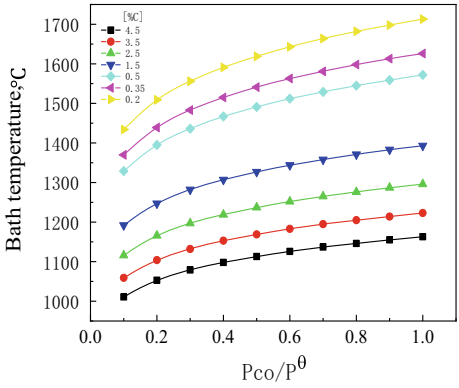

Fig. 3 Equilibrium relationship between CO partial pressure and temperature of carbon and chromium competitive oxidation reaction

conversion temperatures are below 1680 °C. When the content of [C] in molten steel reduces to less than 0.3%, the conversion temperature rapidly increases to above 1680 °C. When the carbon content in molten steel decreases below the critical value, the molten bath temperature cannot meet the temperature requirements of decarburization and chromium reservation, and [Cr] oxidation occurs in molten steel. In this case, to continue decarburization, it is necessary to improve the stirring strength in the furnace and reduce the partial pressure of CO for reducing chromium burning loss in the molten bath.

Under different carbon content conditions, the relationship between CO partial pressure and bath temperature when the carbon and chromium competitive oxidation reaction reaches equilibrium is shown in Fig. 3.

It can be seen from Fig. 3, as the bath temperature increases, the equilibrium partial pressure of CO increases. At a certain temperature, the [C] content of molten steel decreases, and correspondingly, the equilibrium partial pressure of CO decreases rapidly. In addition, as the content of [C] decreases, decarburization and chromium reservation have strict requirements for reducing CO partial pressure.

Determination of Critical Carbon Content

The oxidative reactions of the carbon and chromium can be written as follows:

$$[\mathrm{C}] + \frac{1}{2}\mathrm{O_2} = (\mathrm{CO}) \tag{1}$$

$$\frac{2}{3}[\mathrm{Cr}] + \frac{1}{2}\mathrm{O_2} = \frac{1}{3}(\mathrm{Cr_2O_3}) \tag{2}$$

Combining Eqs. (1) and (2), the decarburization and chromium reservation reaction in AOD refining process of 304 stainless steel can be expressed as Eq. (3):

$$\frac{1}{3}(Cr_2O_3) + [C] = \frac{2}{3}[Cr] + CO \tag{3}$$

When the reaction achieves equilibrium, the equilibrium constant (K_1) can be determined by Eq. (4) [14]:

$$\lg K_1 = \lg \frac{f_{[Cr]}^{2/3}[\%Cr]^{2/3} p_{CO}}{f_{[C]}[\%C]} = -\frac{13114}{T} + 8.38 \tag{4}$$

The activity (a_i) of elements in molten steel can be expressed by Eq. (5):

$$a_i = f_i \cdot [\%i] \tag{5}$$

According to the thermodynamic manual, the activity interaction coefficients of each component to C and Cr ($f_{[C]}$ and $f_{[Cr]}$) in molten steel are found, and they can be calculated by Eqs. (6) and (7), respectively:

$$\lg f_{[C]} = 0.14[\%C] - 0.024[\%Cr] + 0.012[\%Ni] + 0.08[\%Si] - 0.012[\%Mn] \tag{6}$$

$$\lg f_{[Cr]} = -0.12[\%C] - 0.0003[\%Cr] + 0.0002[\%Ni] - 0.0043[\%Si] \tag{7}$$

The activities of carbon and chromium were calculated by Eqs. (5) to (7). Then, by substitute the calculation result into Eq. (4), the following result can be obtained:

$$\begin{aligned} &0.22\%[C] + \lg \%[C] - \lg p_{CO} - 0.024\%[Cr] + 0.012\%[Ni] + 0.08\%[Si] \\ &- 0.012\%[Mn] - 0.67 \lg \%[Cr] = \frac{13,114}{T} - 8.38 \end{aligned} \tag{8}$$

According to Eq. (8), p_{CO} can be obtained by R, and the actual smelting parameters can be substituted into Eq. (8) to obtain the critical carbon content, so as to judge whether the burning loss of chromium occurs in molten steel.

Application of Decarburization and Chromium Reservation Model

Optimization of Gas Supply Parameters

Taking 304 stainless steel produced by 75 t AOD furnace for 3 heats in a stainless steel production enterprise as an example, high oxygen nitrogen ratio ($R = 8.5$) blowing was used in the decarburization stage. The critical carbon content of decarburization period I and decarburization period II was calculated through the model.

Under a certain R, there is a critical carbon content correspondingly. In the actual production process, it is necessary to blow a certain flow of nitrogen (>18 Nm/min) as the protective gas during gas supply. Therefore, the actual value of R has an adjustable range. Correspondingly, there is a controllable range of critical carbon content for decarburization and chromium reservation. The controllable range of critical carbon content of decarburization period I and decarburization period II is shown in Table 1.

It can be seen from Table 1 that when the actual production heats of the 3 heats are blown with $R = 8.5$, at the end of decarbonization period II, the critical carbon contents of the 3 heats are 0.363%, 0.428%, and 0.382%, and the actual carbon contents are 0.110%, 0.093%, and 0.121%, respectively. The carbon content is lower than the critical carbon content. In the decarburization stage, when the carbon content is reduced to the critical carbon content value, the critical carbon content can be reduced by adjusting R online to reduce the burning loss of chromium in molten steel as much as possible.

Before optimizing the blowing parameters, the 75 t AOD converter adopts the gas supply mode of subsection regulation R, namely stepped gas supply, as shown in Fig. 4a. According to the mathematical model of decarburization and chromium reservation and the actual operating conditions, the gas supply mode was optimized as curved gas supply, as shown in Fig. 4b. It can be seen from Fig. 4b, when the

Table 1 Range of relevant gas supply parameters of AOD blowing

Heat	R	Pco/p^{θ}	Critical carbon content, mass pct	End of decarburization period II, mass pct
C02	0.2–8.5	0.429–1.416	0.124–0.363	0.110
C05	0.2–8.5	0.429–1.416	0.149–0.428	0.093
C06	0.2–8.5	0.429–1.416	0.131–0.382	0.121

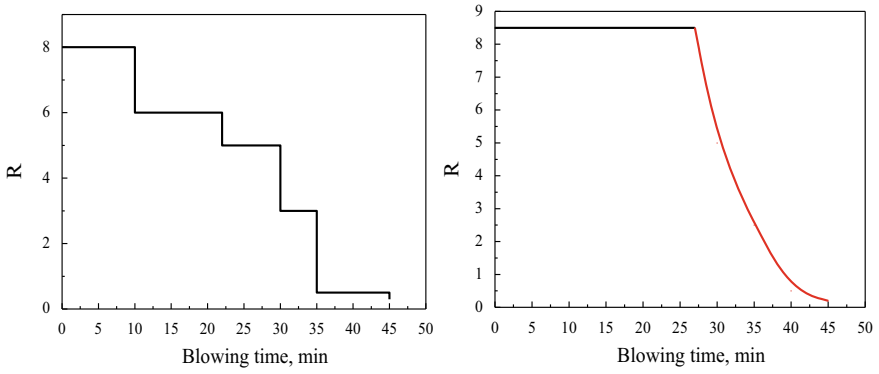

(a) stepped mode (b) curve mode

Fig. 4 Gas supply mode of the AOD blowing

carbon content of molten steel is greater than the critical value, the gas supply adopts a high R. On the contrary, the R is adjusted online, namely curve gas supply.

Model Application Results

In the process of AOD decarburization, the critical carbon content at each sampling point was calculated using the model. In the initial stage of blowing, high R was adopted to improve the decarburization efficiency, which is conducive to a rapid temperature rise of molten bath and shortening smelting cycle. When the carbon content in steel drops to a critical value, the AOD blowing adopts the curve mode of gas supply for decarburization and chromium reservation. In a stainless steel production enterprise, the optimized AOD gas supply scheme was adopted to smelt 10 heats of 304 stainless steel in the 75 t AOD furnace. Compared with 10 heats with similar initial boundary conditions without optimizing gas supply, their relevant production indexes are shown in Table 2.

According to Table 2, compared with the conventional stepped gas supply under similar initial boundary conditions, after optimizing the gas supply parameters, the burning loss of molten steel chromium was significantly reduced, the ferrosilicon consumption of each furnace was reduced, and the smelting cycle was shortened. After optimizing the gas supply parameters, in the initial stage of blowing, the oxygen supply intensity was improved, the decarburization speed was accelerated, and the average smelting cycle was shortened by 6.4 min. In the later stage of blowing, the curve gas supply was adopted. Compared with the conventional gas supply mode, namely stepped mode, the burning loss of chromium was reduced by 1.86%. In the reduction stage, ferrosilicon was added to reduce (Cr_2O_3) in the slag. By optimizing the gas supply parameters, the average consumption of ferrosilicon per heat was reduced by 379.2 kg (34.3%).

Conclusions

In this study, a decarburization and chromium reservation model in AOD refining process of 304 stainless steel was established. By using this model, R adjustment in the refining process was guided, and the optimization of gas supply has achieved good metallurgical results. The following conclusions were drawn: Firstly, according to the theory of competitive oxidation of carbon and chromium, in the process of decarburization in the AOD furnace, increasing the bath temperature and reducing p_{CO} are beneficial to the decarburization and chromium reservation of molten steel. The value of p_{CO} is controlled by R, and adjusting R can achieve the purpose of decarburization and chromium reservation. Secondly, there is a critical carbon content for decarburization and chromium reservation of refining 304 stainless steel

Table 2 Relevant data for refining process of 304 stainless steel 75 t AOD furnace

Heat	Mass of steel, t	End of blowing (Cr_2O_3), Mass Pct	Ferrosilicon consumption, kg	Smelting cycle, min
1	73.5	5.35	1350	95
1’	72.8	2.13	805	78
2	75.6	4.52	1642	86
2’	75	4.30	1350	74
3	78	6.03	1602	90
3’	77.8	2.49	1190	79
4	74	5.64	1410	89
4’	74.7	3.60	1000	89
5	74	4.77	1474	67
5’	74.5	3.56	1015	66
6	72	4.31	1377	78
6’	73.1	2.95	1180	75
7	70	6.07	1236	77
7’	71.9	4.83	1125	71
8	75	5.25	1467	80
8’	74.3	3.73	1096	76
9	76	5.82	1580	83
9’	75.7	3.58	1230	81
10	79	5.13	1695	88
10’	78	3.15	1050	80

1–10: The optimized gas supply of blowing
1’–10’: The conventional gas supply of blowing

in the 75 t AOD furnace. This critical value can be calculated by the decarburization and chromium reservation model, to reduce the oxidation of chromium in blowing. Thirdly, compared with the conventional gas supply mode, the burning loss of chromium can be reduced by 1.86% through optimizing the gas supply parameters, the average ferrosilicon consumption per heat was reduced by 379.2 kg (34.3%), and the average smelting cycle can be shortened by 6.4 min.

Acknowledgements The work supported by the Fundamental Research Funds for the Central Universities (Grant No. FRF-AT-20-13).

References

1. Pariser HH, Backeberg NR, Masson O et al (2018) Changing nickel and chromium stainless steel markets—a review. J South Afr Inst Min Metall 118(6):563–568

2. Chen XR, Cheng GG, Hou YY et al (2019) Oxide-inclusion evolution in the steelmaking process of 304L stainless steel for nuclear power. Metals 257(9):1–11
3. Chen XR, Cheng GG, Hou YY et al (2020) Influence of refining process and utilization of different slags on inclusions, titanium yield and total oxygen content of Ti-stabilized 321 stainless steel. J Iron Steel Res Int 27(8):913–921
4. Kim WY, Nam GJ, Kim SY (2021) Evolution of non-metallic inclusions in Al-killed stainless steelmaking. Metall Mater Trans B 52(3):1508–1520
5. Wei W, Gustavsson J, Samuelsson PB et al (2021) Prediction of nitrogen behaviour in the AOD process by a time-dependent thermodynamic model. Ironmaking Steelmaking 1–13
6. Mani C, Karthikeyan R, Davim JP (2020) A review on austenitic stainless steel-based dissimilar metal welding using gas tungsten Arc welding. J Manuf Technol Res 12(1/2):65–82
7. Liu YL, Guo GC, Bin H et al (2018) Formation of non-metallic inclusions of Si-killed stainless steel during GOR refining process. High Temp Mater Processes (London) 37(6):521–529
8. Andersson N, Tilliander A, Jonsson LTI et al (2012) Investigating the effect of slag on decarburization in an AOD converter using a fundamental model. Steel Res Int 84(2):169–177
9. Andersson N, Tilliander A, Jonsson L, Jönsson PG (2012) An in-depth model-based analysis of decarburization in the AOD process. Steel Res Int 83(11):1–14
10. Deo B, Kumar S (2013) Dynamic on-line control of stainless steel making in AOD. Adv Mater Res 794:50–62
11. Wei JH, Zhu DP (2002) Mathematical modeling of the argon-oxygen decarburization refining process of stainless steel: part I. Mathematical model of the process. Metall Mater Trans B 33(1):111–119
12. Pisilä SE, Järvinen MP, Kärnä A et al (2011) Fundamental mathematical model for AOD process: part II: model validation. Steel Res Int 82(6):650–657
13. Wei JH, Zhu DP (2002) Mathematical modeling of the argon-oxygen decarburization refining process of stainless steel: part II. Application of the model to industrial practice. Metall Mater Trans B 33(1):121–127
14. Chen C (2005) Application of the selective oxidation in carbon elimination and chromium conservation of stainless steel. Sci/Tech Inf Dev Econ 58(2):40–46(7)